Numerical and experimental investigation of early iron particle formation in $Fe(CO)_5$ doped premixed $H_2/O_2/Ar$ flames at low pressure

L. Deng[1], S. Kluge[2], N. Sikalo[1], O. Hasemann[1,3], H. Wiggers[2,4], C. Schulz[2,3,4], A. Kempf[1,3,4], I. Wlokas[1,3]

[1]IVG, Institute for Combustion and Gas Dynamics – Fluid Dynamics, Duisburg, Germany
[2]IVG, Institute for Combustion and Gas Dynamics – Reactive Fluids, Duisburg, Germany
[3]CCSS, Center for Computational Sciences and Simulation, Duisburg, Germany
[4]CENIDE, Center for Nanointegration Duisburg-Essen, Duisburg, Germany

Abstract

A premixed, laminar $H_2/O_2/Ar$ low-pressure flat flame doped with iron-pentacarbonyl ($Fe(CO)_5$) was used to investigate the formation of nanoparticles. The particles were extracted from the flame using a molecular beam sampling probe, the mass flow rate of condensable material was measured by a quartz crystal microbalance. It was observed that particles are already formed on the cold side of the flame, and vanish quickly once they pass through the flame front. To understand the process and assess the perturbations caused by the sampling probe, simulations of the synthesis flame, the reactor, and the sampling were carried out. The simulations confirmed the experimental findings and the detailed knowledge of the perturbation caused by invasive probing enabled further tuning of the iron oxide formation mechanism.

Introduction

Flame-assisted synthesis is a convenient way to produce gas borne, nano-sized metal-oxide particles. The process path is very attractive for industrial applications, but scaling from the lab-scale to industrial-scale requires a detailed understanding of the reaction kinetics. A frequently used precursor for the production of iron-oxide from laminar, low-pressure flames is iron-pentacarbonyl ($Fe(CO)_5$), due to its relatively high vapor pressure. The low-pressure, laminar flat flame enables spatially resolved measurements of flame species and particles using molecular beam sampling.

Iron-pentacarbonyl as an additive in flames has been investigated since the 1920's, when it was applied as an anti-knock agent. It was observed that nearly any addition of $Fe(CO)_5$ strongly affects the flame's reaction kinetics. An overview of recent publications on iron-containing compounds in flames was given by Wlokas et al. [1]. They also proposed a mechanism for iron-oxide formation from the gas phase in the post-flame region. In their mechanism, due to lack of experimental evidence, formation of iron clusters was completely neglected. Cluster formation by pyrolysis of $Fe(CO)_5$ was described by Giesen et al. [2] and later, in more detail by Wen et al. [3],

Recently, early iron particle formation has been observed by Feroughi et al. [4] in a non-premixed $Fe(CO)_5$ doped CH_4/O_2 flame. The authors proposed a reaction mechanism, based on the iron-oxide formation by Wlokas et al. [1] and the iron-cluster formation mechanism by Wen et al. [3], to confirm the hypothesis of iron-cluster formation on the fuel rich side of the non-premixed flame. Very recently, Poliak et al. [5] presented evidence for the formation of particles in the pre-flame region of a premixed $Fe(CO)_5$ doped CH_4/O_2 flame. They measured the deposition of particulate material using a particle mass spectrometer combined with a quartz crystal microbalance (PMS-QCM) as proposed by Fomin et al. [6]. Their measurements and the hypothesis of early iron-cluster formation could be qualitatively confirmed by one-dimensional simulations of the doped flame using the mechanism proposed by Feroughi et al. [4].

To spatially resolve the particle concentration in the flame, a molecular-beam sampling technique was applied. This method is widely used for the investigation of flames and spatial profiles of the gas composition or the particle mass can be obtained. Usually, the premixed, laminar, flat flame is is assumed to be one-dimensional. However, the method is invasive and the probe causes thermal and aerodynamic perturbations that violate the one-dimensionality of the flame. Although many methods for correcting the data measured in the perturbed flame were proposed, two- or three-dimensional simulations of the reacting flow provide the most detailed picture of the sampling effect. For sampling in low-pressure flames the effect was investigated by Gururajan et al. [7], while Deng et al. [8] investigated sampling from atmospheric flames. Deng also demonstrated the suitability of the detailed two- and three-dimensional simulations for quantification of the flow, temperature and species concentration fields in the flame. Complementary to the simulations in 2-D/3-D with reduced reaction kinetics, 1-D simulations with detailed mechanism and reconstructed flow and temperature field were conducted. In the present paper this simulation work-flow [8] was applied in the context of particle sampling for validation of the reaction mechanism and of the hypothesis on early iron-particle formation.

In this work we demonstrate the combination of experimental methods and state-of-the-art flow simulation to reconstruct the experimentally inaccessible flow field quantities. The combined PMS-QCM technique was used to close the gap in detection of condensable mater between the burner surface and the area of formation of

* Corresponding author: lei.deng@uni-due.de
Proceedings of the European Combustion Meeting 2011

first detectable iron-oxide nanoparticles. The modeling and the experimental results confirmed the observations made by Feroughi et al. [4] and by Poliak et al. [5] regarding the prompt formation of iron particles upstream of the flame. The skeletal mechanism, derived from the mechanisms proposed by Feroughi et al. was shown to be suitable for simulations of laminar flames in complex flow geometries. The detailed knowledge of the perturbation caused by the invasive probing enabled further improvement of the iron-oxide formation mechanism.

Experiment

Iron oxide nanoparticles were synthesized through the decomposition of iron-pentacarbonyl $Fe(CO)_5$ in a premixed H_2/O_2 flame diluted by argon. An almost one-dimensional, low-pressure flat flame burning in an upwards direction is operating at 30 mbar to spatially extend the reaction zone. At various locations downstream of the burner head small samples of the aerosol are expanded through a sonic nozzle and a skimmer (both Beamdynamics Model 2, 0.5 mm opening diameter) into high vacuum to form a particle-laden molecular beam. The decomposition of the precursor and its influence on the flame chemistry can be studied by varying the distance between the burner head relative to the nozzle position (HAB: height above the burner) which represents the residence time within the reactor. A sketch of the experimental setup is given in Fig. 1.

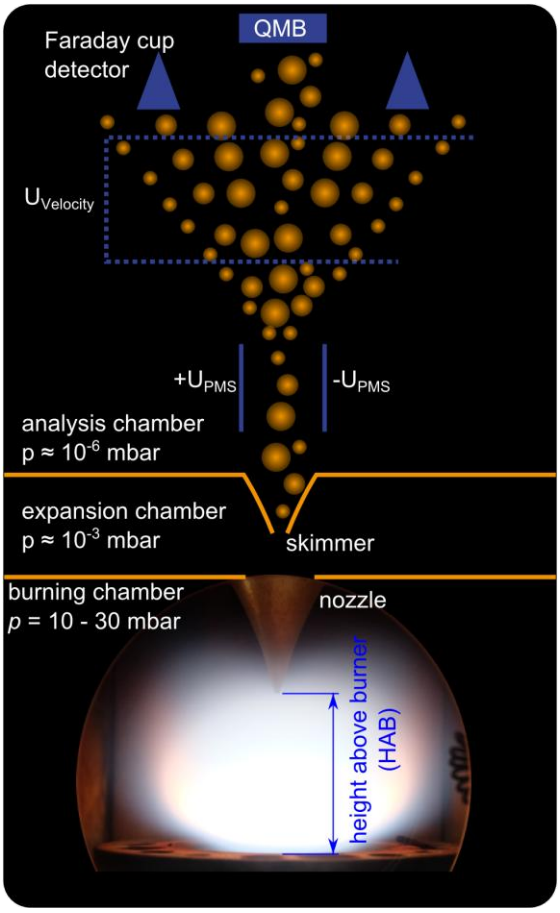

Figure 1: Experimental setup

By replacing parts of the argon flow with a flow of $Fe(CO)_5$ diluted in argon, the precursor concentration was varied between 0 and 750 ppm.

To detect condensable species inside the molecular beam, a quartz crystal microbalance is centered on the axis of the beam. The deposition of material on the gold-coated quartz crystal shifts its resonance frequency proportionally to the deposited mass. For each parameter set (HAB, ppm) the resonance frequency of the quartz crystal has been measured for 60 s. The slope of the frequency versus time graph is proportional to the mass deposition rate. For a given precursor concentration measurements were carried out for various HAB.

The nanoparticle synthesis reactor setup employed in this work was first introduced for similar investigations by Janzen et al. [9] for PMS measurements and by Hecht et al. [10] for Fe-atom LIF measurements. In contrast to the previous investigations with a horizontal flow direction, the orientation of the reactor is now "upright", following the recommendations given by Weise et al. [11]. The main reactor chamber has a diameter of 100 mm with four windows enabling optical access. The burner plate has a diameter of 36 mm and is cooled by water at a temperature of 300 K. The fresh gas, constituting 400 sccm H_2, 400 sccm O_2 and 600 sccm Ar, is fed into the burner through a porous metal plate. In the measurements, the sampling probe, made of nickel with an orifice diameter of 0.5 mm, was positioned along the axis of the flame between 0 and 10 mm above the burner surface.

Modeling approach

The reacting flow was described by the conservation equations for mass, momentum, energy and species. The mixture-averaged model for the diffusion of individual species properties was implemented into this framework due to the satisfactory accuracy and low computational effort. The laminar viscosity of the mixture was calculated from the equation developed by Wilke [12]. The thermal diffusivity was considered as a fraction of thermal conductivity and heat capacity at constant pressure. The thermal conductivity was calculated following the equation introduced by Mathur et al. [13] and the heat capacity at constant pressure was treated in a mass fraction averaged formulation.

The simulation framework is based on the open source CFD software OpenFOAM [14]. The software model extensions and numerical methods were described in detail by Deng et al. [8].

The CFD simulations are computationally very expensive and thus performed usually using a reduced, skeletal reaction mechanism. The error introduced by such reduced mechanisms affects mostly the resulting species concentrations while the velocity and temperature fields are predicted with high reliability. We have hence used a combined two-step approach: We first simulated the reactor in two dimensions (OpenFOAM) with reduced chemistry, correcting the results with detailed chemistry calculations from 1-D simulations along a stream line [8] using Cantera [15].

The presence of iron atoms strongly affects the flame chemistry. In lean conditions at low pressures a flame-promoting effect is observed with an increased heat release from the flame [16]. To capture these effects, the main reaction paths of flame radical and metal species interaction must be included in the reaction mechanism. For our simulations the sub-mechanism of iron-pentacarbonyl reactions, first introduced by Feroughi et al. [4] for $Fe(CO)_5$ doped CH_4/O_2 flames, was merged with the C1 mechanism by Li et al. [17]. The resulting mechanism contained 50 reacting species and 227 reactions. The reduced, skeletal mechanism employed for the CFD simulations was derived from it using a genetic algorithm method proposed by Sikalo et al. [18] and contained 40 species and 66 reactions. The reduced mechanism was validated for laminar flame speeds, adiabatic flame temperatures, total iron-cluster mole fractions and the molar fraction of iron oxide.

Simulation

The flat flame burner was confined by a steel housing. A detailed simulation requires usually considerations of all geometric effects. Here, a quasi 2-D rotationally-symmetric computational domain was found to be sufficient to capture the influence caused by the housing of the reactor. Figure 2 shows a "to scale" sketch of the computational domain on the right side and a picture of the reactor, including the burner and the probing nozzle, on the left side.

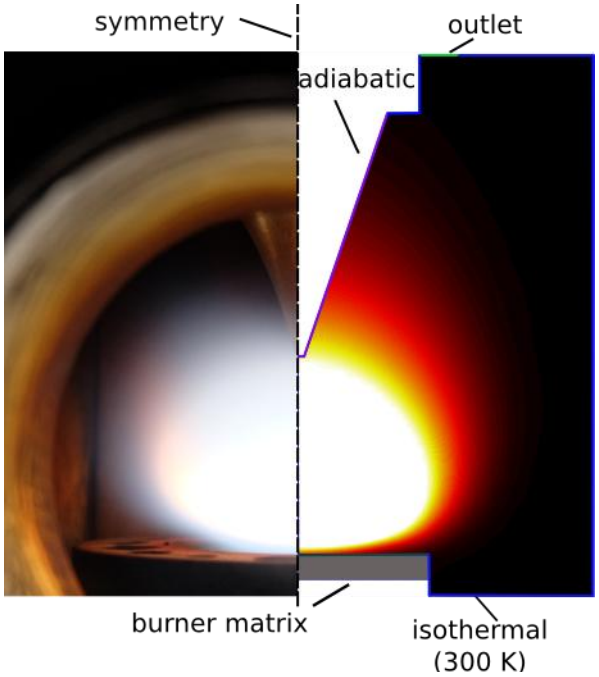

Figure 2: The reactor burner (left) and the corresponding computational geometry.

It was expected that the relatively large probe would strongly perturb the flame. To capture these perturbations, simulations were carried out for five probe positions in steps of 2 mm from 2 to 10 mm HAB. The probe, made of Nickel, was assumed to be adiabatic [8]. The outer boundary was isothermal at $T = 300$ K mimicking the heat losses through the reactor housing.

Results and discussion

Experimental results

The flame was scanned for HAB positions from 1 to 9 mm in steps of 1 mm. The duration of each sampling was 60s. Figure 3 shows normalized sampled mass of condensable particle material as a function of HAB. The increase in the particle mass as a function of $Fe(CO)_5$ concentration is consistent with the findings by Poliak et al. [5]. However, the measurements at high $Fe(CO)_5$ concentrations of 500 and 750 ppm show maximum values that are lower than expected, compared to the masses observed at lower concentrations. The reason was found to be clogging of the sampling nozzle by particles.

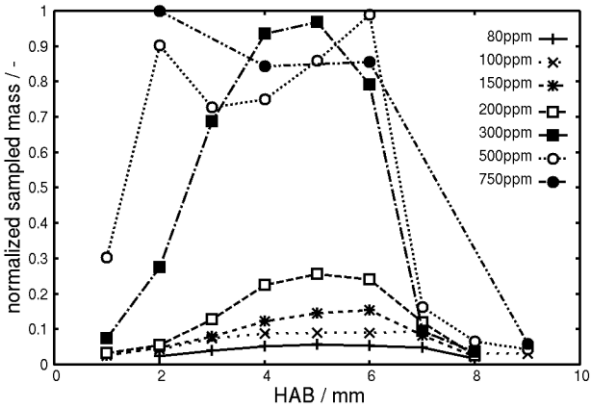

Figure 3: Normalized sampled mass of particles in the synthesis flame at low HAB; the sampling time is limited due to clogging of the nozzle at high $Fe(CO)_5$ concentrations.

Numerical Simulation

In a first step we investigated the effect of the addition of iron-pentacarbonyl to the fresh gases without the invasive probing. The simulations showed a strong increase in temperature, caused by recombination reactions of flame radicals and Fe-species, and confirmed former observations [1]. Figure 4 shows the difference in temperature between the undoped and the doped flame.

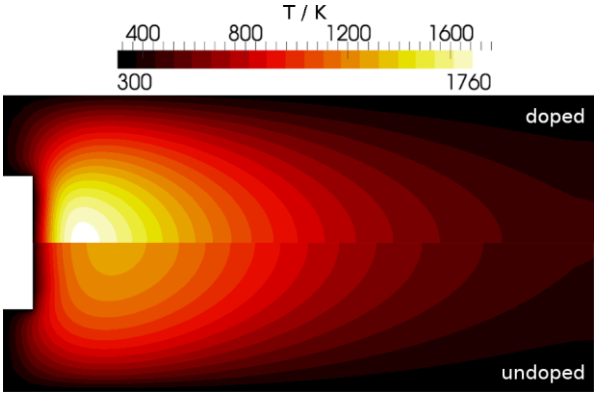

Figure 4: Temperature distribution for the investigated flame undoped (bottom) and doped (top) with 300 ppm $Fe(CO)_5$.

The resulting temperature profiles at the reactor axis, together with the molar fractions of iron oxide and the

accumulated iron clusters $Fe_{2\sim8}$ are shown in Fig. 5 for the three investigated cases. Due to the low concentration of iron clusters, the succeeding simulations of the probe perturbed flow were carried out for flames doped with $Fe(CO)_5$ concentrations of 300, 500 and 750 ppm.

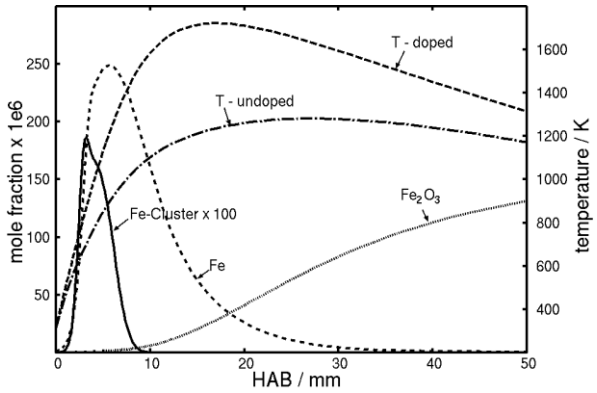

Figure 5: Temperatures of the doped and the undoped flame along the axial stream line. The iron particles are represented as accumulated mole fraction (×100 ppm) of iron-clusters.

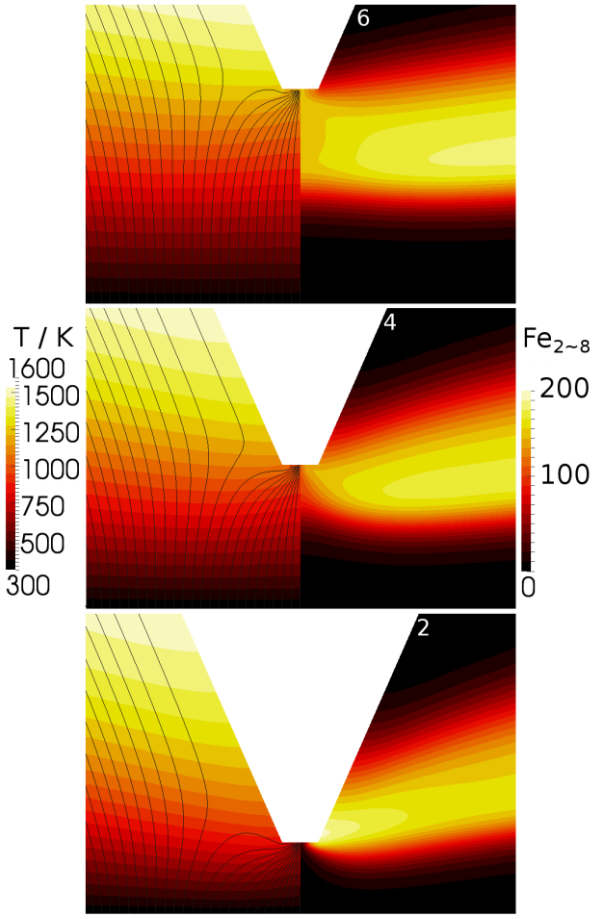

Figure 6: Streamlines, temperature (left) and the accumulated Fe-cluster mole fraction (right, ×100 ppm) at probe positions of 2, 4 and 6 mm HAB. The presence of the probe leads to a strong deviation from one-dimensionality of the flame illustrated by the streamlines and the Fe-cluster profile.

An example for the strong perturbation of the flame by the probe is shown for positions of 2, 4 and 6 mm HAB in Fig. 6. At low HAB, the flame is "pushed" towards the burner surface, while at higher HAB, the flame is "lifted". This effect leads to an apparent thickening of the flame – the perturbed flame appears thicker than it really is. Moreover, the large orifice diameter causes a large zone of flow acceleration, illustrated by the flow stream lines. The normalized mass flow rate through the orifice of the probe was calculated in all simulations. Comparison with the experimentally obtained particle mass profiles showed a good and plausible agreement, displayed in Fig. 7. The normalization is required for two reasons: first, the sampling efficiency of the combined PMS-QCM apparatus is unknown and second, the sub-mechanism of Fe-cluster formation is not quantitatively validated for flames.

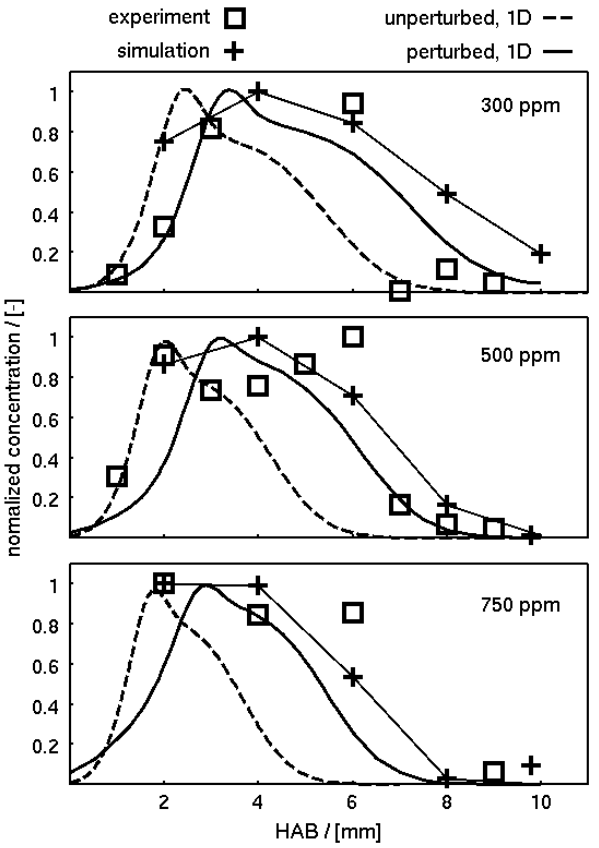

Figure 7: Normalized Fe-cluster concentration from experiment (boxes), 2-D simulation of the sampling (crosses) and from 1-D simulations (lines).

The Fe-cluster formation was investigated with the detailed reaction mechanism for one-dimensional flames using the temperature profile of the adiabatic, unperturbed flame and the temperature profile reconstructed from the 2-D simulation at HAB = 10 mm. The normalized Fe-cluster profile obtained from simulations with the perturbed temperature showed the expected thickening of the flame by lifting (solid line, Fig. 7). The simulation of the unperturbed flame did not resemble the measured Fe-cluster (Fe-particle) profiles (dashed line, Fig. 7). Nevertheless, the probe effects

could be compensated only partially for the conditions at the axis, while the contour plot shows a strong deviation from one-dimensionality.

Conclusions

The presented experimental results of early particle formation in an iron-pentacarbonyl doped premixed $H_2/O_2/Ar$ flame confirmed the findings by Poliak et al. [5] made for a nanoparticle producing CH_4/O_2 flame of similar geometry. The measurements at low dopant concentrations were in good agreement, while the measurements at high concentrations suffered from clogging of the probe's orifice. The clogging can be possibly avoided by reducing the sampling time in future experiments.

The developed skeletal mechanism of $Fe(CO)_5$ in flames was found to be suitable for application in 2-D or 3-D simulations of a reacting flow. It predicts the temperature, Fe-atom concentration, and Fe_2O_3 particle-precursor formation with good accuracy. The formation of Fe-particle precursors (cluster) could be validated for plausibility.

The 2-D simulations of the doped flame, based on the skeletal mechanism, resembled the measured profiles of the particle mass assuming the formation of Fe-clusters.

The 2-D flow simulation is not suitable for the, iterative use in the optimization of reaction mechanism, as the computational cost would be too high. In turn, 1-D models are more affordable, but cannot compensate for the considerable probing effect as demonstrated in this work. Temperature profiles from 2-D simulations were shown to be reliable, but an exhaustive reconstruction of an experiment will require individual simulations for every single data-point.

Acknowledgement

CS and HW acknowledge funding by the German Research Foundation under SCHU1369/13.

References

1. I. Wlokas, A. Faccinetto, B. Tribalet, C. Schulz, A. Kempf, *Int. J. Chem. Kinet.* 45 (2013) 487-498.
2. A. Giesen, J. Herzler, P. Roth, *J. Phys. Chem. A* 107 (2003) 5202-5207.
3. J.Z. Wen, C.F. Goldsmith, R.W. Ashcraft, W.H. Green, *J. Phys. Chem. C* 111 (2007) 5677-5688.
4. O.M. Feroughi, S. Hardt, I. Wlokas, T. Hülser, H. Wiggers, T. Dreier, C. Schulz, *Proc. Combust. Inst.* 35 (2015) 2299–2306.
5. M. Poliak, A. Fomin, V. Tsionsky, S. Cheskis, I. Wlokas, I. Rahinov, *Phys. Chem. Chem. Phys.* 17 (2015) 680-685.
6. A. Fomin, M. Poliak, I. Rahinov, V. Tsionsky, S. Cheskis, *Combust. Flame* 160 (2013) 2131-2140.
7. V. Gururajan, F.N. Egolfopoulos, K. Kohse-Höinghaus, *Proc. Combust. Inst.* 35 (2015) 821–829.
8. L. Deng, A. Kempf, O. Hasemann, O.P. Korobeinichev, I. Wlokas, *Combust. Flame* (2014) 10.1016/j.combustflame.2014.11.035.
9. C. Janzen, P. Roth, *Combust. Flame* 125 (2001) 1150-1161.
10. C. Hecht, H. Kronemayer, T. Dreier, H. Wiggers, C. Schulz, *Appl. Phys. B* 94 (2009) 119-125.
11. C. Weise, A. Faccinetto, S. Kluge, T. Kasper, H. Wiggers, C. Schulz, I. Wlokas, A. Kempf., *Combust. Theory Mod.* 17 (2013) 504-521.
12. C.R. Wilke, *J. Chem. Phys.* 18 (1950) 517-519.
13. M.S. Mathur, S.C. Saxena, *Appl. Sci. Res.* 17 (1967) 155-168.
14. OpenCFD OpenCFD release OpenFOAM. http://www.openfoam.org/version2.1.0
15. D. Goodwin Cantera: An object-oriented software toolkit for chemical kinetics, thermodynamics, and transport processes. http://code.google.com/p/cantera
16. G.T. Linteris, V.I. Babushok, *P. Combust. Inst.* 32 (2009) 2535-2542.
17. J. Li, Z. Zhao, A. Kazakov, M. Chaos, F.L. Dryer, J. J. J. Scire, *Int. J. Chem. Kinet.* 39 (2007) 109-136.
18. N. Sikalo, O. Hasemann, C. Schulz, A. Kempf, I. Wlokas, *Int. J. Chem. Kinet.* 46 (2013) 41-59.